Systematic Method to New Phases of Polymeric Nitrogen under High Pressure

F. Zahariev,[1] S. V. Dudiy,[1] J. Hooper,[1] F. Zhang,[2] and T. K. Woo[1]

[1]*Department of Chemistry, University of Ottawa, D'Iorio Hall, Ottawa, Ontario, K1N 6N5, Canada*

[2]*Defence R&D Canada-Suffield, PO Box 4000, Medicine Hat, Alberta T1A 8K6 Canada*

(Received 22 February 2006; published 13 October 2006)

A systematic method to unravel a large class of single-bonded (SB) polymeric phases of nitrogen under high pressure is presented. The approach is based on the combinatorial generation of different Peierls-like distortions of a given reference structure that maintain the threefold connectivity of SB nitrogen, followed by first-principles calculations. Using an eight atom simple cubic reference structure, the approach not only recovers all four SB nitrogen phases reported to date, but eight new metastable structures (confirmed by phonon density of states calculations) are found. Basic properties of the structures are computed and the trends analyzed. Extensions to the method are straightforward and should lead to the discovery of more phases of polynitrogen.

DOI: 10.1103/PhysRevLett.97.155503 PACS numbers: 61.50.Ah, 61.50.Ks, 62.50.+p, 71.15.Mb

Nonmolecular, polymeric nitrogen composed solely of single bonds, in analogy to carbon in diamond, has long been thought to exist at high pressures. If such a material were metastable at ambient pressures, it would make an extremely powerful high-energy-density material (HEDM), for use in energy storage systems, propellants, and explosives. Because of the uniquely large difference in energy between the N-N single and triple bonds, the energy density of single-bonded polymeric nitrogen has been calculated [1] to be at least 0.4 $\mathrm{eV/cm^{-1}}$, which is about 3 times that of the most powerful energetic materials known today.

The structure of single-bonded polymeric nitrogen was at first suggested to be that of the known single-bonded forms of nitrogen's group 15 congeners, namely, the black phosphorus (BP) structure and the A7 structure of arsenic. Then in 1992, Mailhiot, Yang, and McMahan [2] predicted that a unique single-bonded form of polymeric nitrogen, not seen in any other element, might exist at high pressure. The newly termed *cubic gauche* (CG) structure was predicted to be more stable than the BP and A7 phases based on first-principles calculations. Following this pioneering work, further computational studies [3] showed that CG might be metastable at ambient pressures, thereby furthering the prospect of using polymeric nitrogen as a practical HEDM.

Experimentally, there have been extensive efforts to produce polymeric nitrogen, and recently, evidence for nonmolecular amorphous phases of nitrogen at high pressure have been reported [4–6]. In one such study [4], the amorphous material was even recovered at ambient pressures and low temperature. However, in these studies there was no convincing evidence for the cubic *gauche* phase or any other purely single-bonded form with an extended polymeric structure [7]. Rather, it is likely that the amorphous materials observed were mixtures of small clusters of nonmolecular phases.

Finally in 2004, Erements and co-workers reported [7] that they were able to synthesize a crystalline form of single-bonded polymeric nitrogen. With pressures greater than 110 GPa and 2000 K temperatures, molecular nitrogen was transformed into the long sought after *cubic gauche* crystal structure. It is possible that other metastable phases of polymeric nitrogen could be reached via yet unexplored experimental paths that may be more stable at ambient pressures or easier to synthesize.

Recently, a number of new phases of polymeric nitrogen have been found by first-principles molecular dynamics (MD) calculations in which high pressures and temperature conditions are simulated [8–10]. Alemany and Martins [9] found a metastable metallic phase composed of zigzag chains of nitrogen atoms packed in a body-centered orthorhombic structure. Through similar MD simulations using temperatures up to 10 000 K, Martin and co-workers [8] also discovered a metastable nonmolecular phase composed of zigzag chains. However, a different packing arrangement resulted in a phase with significantly lower energy. Although not single bonded, this new zigzag phase is lower in energy than CG at low pressures and competitive with CG at higher pressures. Using first-principles MD, we have also discovered a new purely single-bonded phase of nitrogen with a layered boat (LB) structure [10]. Although successful, the search for new phases by first-principles MD simulations is *ad hoc* in nature and very computationally demanding. A systematic method to finding new polymeric nitrogen phases is obviously desirable and the fact that all single-bonded metastable phases of group 15 elements predicted or found in nature can be considered Peierls-like distortions of the simple cubic (SC) structure hints at such a method.

In this Letter we present a systematic search for purely single-bonded allotropes of polymeric nitrogen. The method is a synthesis of modern first-principles calculations with the geometrical model of crystal structure developed by Wells [11], Adams [12], and Burdett [13,14]. In contrast to other general structure prediction frameworks, such as the ''quotient graph'' technique [15] or tilling surfaces of negative curvature [16] used to search for new carbon phases, our procedure more effectively ex-

ploits the connection to the SC reference structure, allowing us to focus on the most physically meaningful structure candidates. The procedure is not only able to recover all of the threefold connected allotropes found so far (A7, BP, CG, and LB), but eight new single-bonded allotropes of nitrogen are found whose metastability is confirmed by phonon calculations.

We consider the high-pressure metastable allotropes of nitrogen as distortions of a given reference structure. Experimental observations distinguish SC to be the natural high-pressure reference structure for group 15 elements. For example, although at ambient conditions arsenic is a rhombohedral crystal (A7), and phosphorus forms an orthorhombic crystal (BP), the SC structure is favored for both at high pressures. Specifically, BP phase of phosphorus first undergoes a structural transition to A7 at 5 GPa and at an even higher pressure of 10 GPa to SC [17]. Arsenic transforms directly to SC from A7 at high pressure. After a gradual release of pressure the SC phase transforms back to A7 phase, followed by BP phase for phosphorus [17]. The distortion of SC with lowering the pressure is regarded either as a Peierls/Jahn-Teller type effect and/or an effect triggered by s-p orbital hybridization.

The approach presented here is based on Peierls-like distortions of the SC reference structure in order to systematically generate new polynitrogen structures. However, in order to generate single-bonded structures, the distortions must be consistent with a threefold connectivity pattern of nitrogen. In the undistorted SC structure, each nitrogen atom has 6 nearest neighbors that are equidistant from it. The distortion must be such that each nitrogen atom forms only 3 covalent bonds, thereby breaking 3 of the ''bonds'' of the original SC structure. To obtain a complete set of possible SC distortions consistent with threefold connectivity, we use the combinatorial analysis procedure of Burdett and McLarnan [13], which is based on a generalization of Polya's enumeration theorem [18]. In particular, Burdett and McLarnan's work shows that out of 4096 possible combinations there are only 36 unique ways of labeling the edges of an 8 atom SC unit cell as ''bonds'' and ''nonbonds,'' consistent with the threefold connectivity. Those bond-breaking patterns can be described by connectivity diagrams or structure types, as depicted in Fig. 1. The complete specification of all of the 36 structure types is provided in Ref. [13], and throughout the Letter we adhere to the same numbering. Note that all of the previously reported structures of single-bonded nitrogen, such as CG, BP, A7, and LB, are covered by that set of 36 structure types. Figure 1 shows the connectivity diagrams for BP (structure #1), CG (#3), and a new structure #11 that will be discussed in further detail later in the Letter.

Once a structure type is chosen, the next step in the procedure is to use the connectivity pattern to distort the SC structure as to generate an initial geometry that can be further refined by first-principles optimizations. The most straightforward distortion is to displace each atom of the unit cell by a distance, d, along the body diagonal toward

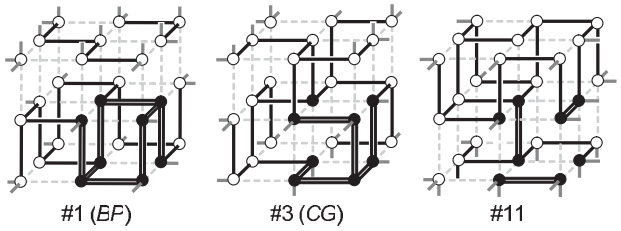

FIG. 1. Connectivity diagrams of a simple cubic reference structure consistent with a threefold coordination of nitrogen. Shown are the connectivity diagrams of structure #1, #3, and #11 of a possible 36. A single 8 atom SC unit cell is highlighted with black atoms and striped bonds.

the three nearest neighbors with which it is to form a bond as shown in Fig. 2(b). Once all atoms are distorted in this way, a rough initial structure is generated as depicted in Fig. 2(c). This can be described as a Peierls-like distortion of the SC structure. This initial structure acts as a starting point for a series of first-principles calculations. In this work, we have utilized Kohn-Sham density functional theory calculations with the Perdew-Burke-Ernzerhof (PBE) exchange-correlation functional [19]. The Vienna *ab initio* simulation package (VASP) [20] was used with the projector augmented wave (PAW) method of Blöchl [21] to treat the core states. A plane-wave cutoff of 39 Ry was used and Brillouin-zone integration was performed using a Monkhorst-Pack grid of $8 \times 8 \times 8$.

Although first-principles optimization of the initial structures may seem straightforward, the considered structures may not be stable at all pressures, if at all. Thus, a careful structure optimization procedure is needed in order to find the appropriate ranges of pressure or volume conditions, as well as to prevent premature decomposition of structures before they get sufficiently close to the final optimized geometries. Here we adopted the following computational procedure. Beginning with the initial structure generated by the aforementioned Peierls-like distortion, the lattice constant a is scanned from 4.1 Å downwards, with a step of 0.05 Å. For each value of a, the following optimization steps are performed. First the distortion parameter d is adjusted to minimize the *ab initio* calculated total energy. Then we allow relaxation of the

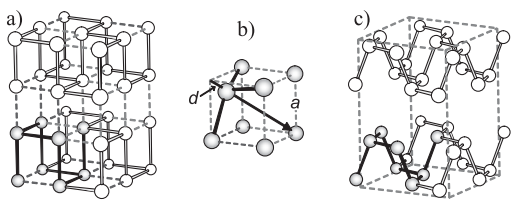

FIG. 2. Schematic illustration of the procedure. (a) A structure type of an eight atom cube is first chosen. A Peierls-like distortion that is consistent with the connectivity is applied. (b) shows the distortion performed on a single atom of a single unit cell, whereas (c) shows the structure after distortion of all atoms in an extended representation.

unit cell shape, fixing the fractional coordinates of the atoms and the unit cell volume. Finally, we perform full relaxation of both the unit cell shape and the atomic positions at fixed unit cell volume a^3. At each such relaxation stage we check whether the structure still preserves the intended connectivity pattern. The scan of the lattice constant continues until either the first time we encounter a fully optimized structure with a required connectivity pattern or reach $a = 3.0$ Å. In cases where we arrive at a fully optimized structure that preserves the intended structure type, which happened for 26 out of 36 types, we check mechanical stability of that structure by calculating its phonon spectrum, and we also calculate its enthalpy-pressure curve. The phonon densities of states for each of the 26 structures at pressures considered (see the auxiliary electronic material [22]) are deduced from a force constant matrix calculated in a $2 \times 2 \times 2$ (64 atom) supercell by means of consecutive displacements of each atom of the original unit cell by 0.02 Å along each axis. Because of the large number of phonon calculations required, a larger supercell could not be used for the phonon calculations with the computational resources available. In some cases the supercell size may be inadequate, giving rise to false negative frequencies [23]. In this respect, only the affirmative outcomes of our metastability tests should be treated as conclusive. To calculate the enthalpy-pressure curve, the volume of the initially obtained fully optimized structure is changed by either a small increment or decrement, and the structure is fully reoptimized at the new volume. The structures optimized at the new volumes are then used as starting points in further gradual volume changes and structural optimization. The range of volumes (and the corresponding pressures) is extended until either the structure is not preserved during relaxation or it goes beyond the 0–300 GPa pressure range. The results of our calculations are shown in Figs. 3–5.

Among all structures studied, the cubic *gauche* phase is still clearly the lowest-enthalpy structure over the whole pressure range studied, and it also shows pronounced mechanical stability in our phonon calculations, which is consistent with the same type of analysis in Ref. [3]. Leaving the cubic *gauche* case aside, our data in Fig. 3 suggest that some structures that have never been considered in the context of single-bonded nitrogen, such as structure types #8 and #11, have enthalpies that are comparable to or lower than those of the previously studied structures #1 (BP), #7 (A7), and #15 (LB). This is particularly clear in the enthalpy-pressure curves of those selected structures in Fig. 5.

To get an insight into the relative energy rankings of different structure types, we analyze a correlation between the first-principles total energies and the number of *cis*, *gauche*, *trans* dihedral angles, and 4-membered rings of those structure types. Based on such analysis, we can interpret the lowest energy structures of the low pressure region, structures #3 (CG) and #11 (new), as structures that minimize the number of *trans* dihedrals and 4-membered

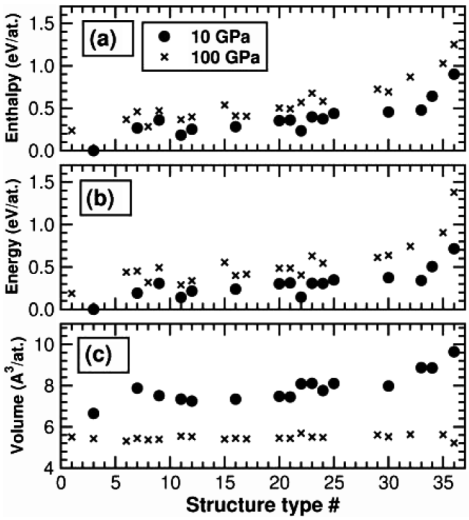

FIG. 3. Calculated (a) enthalpy, (b) total energy, and (c) volume per atom vs structure type # at pressures of 10 GPa (●) and 100 GPa (×). The enthalpies and energies are with respect to those of the CG phase at the corresponding pressures. Note that structures #1, 3, 7, and 15 are the previously known phases—BP, CG, A7, and LB, respectively.

rings while maximizing the *gauche* dihedrals. It is interesting to note that the larger energy penalty due to the *trans* dihedrals compared to the *cis* dihedrals is in contrast with the simplified "lone-pair" orbital picture [2,14] gained from *ab initio* calculations on small nitrogen molecules.

Analysis of the mechanical stability, via a phonon density of states calculation, of all single-bonded structures, resulted in at least 8 of the 26 new structures being mechanically stable at pressures less than 100 GPa (#6, 8, 9, 11, 16, 20, 21, and 30). Structures #11 and 30 are even found to be mechanically stable at zero pressure.

After mechanical stability screening, our newly found structures #11 and #8 are the second lowest-enthalpy structures after cubic *gauche* at low ($<$40 GPa) and moderate-high ($\gtrsim$40 GPa) pressures, respectively. Selected views of structures #11 and #8 are shown in Fig. 6(a) and 6(b), respectively. Structure #11 is distinguished by the high R_{32} symmetry and its structure can be described by two

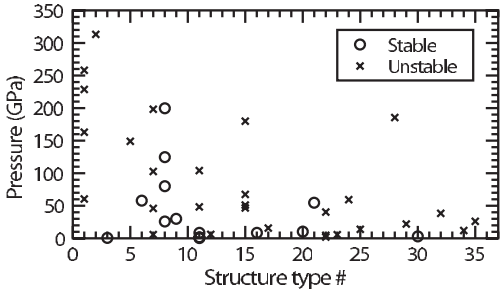

FIG. 4. Results of the phonon spectra based mechanical stability tests. The plot shows for what structure types (x axis) and at what pressures (y axis) we find mechanical stability (○) or instability (×).

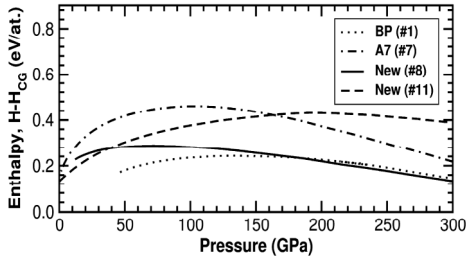

FIG. 5. Enthalpy vs pressure curves of the two lowest-enthalpy structures among the newly found structures compared to the previously studied BP and A7 structures. The enthalpies at each pressure are with respect to the enthalpy of the CG phase at the same pressure.

mutually orthogonal sets of *cis-trans* chains directed along the three coordinate axes (optimized geometries of all 8 new metastable phases are provided in the auxiliary electronic material [22]). Structure #8 has P_{-1} symmetry. It has a very strong structural resemblance to structure #11, being similarly shaped by sets of *cis-trans* chains but just along two out of the three axes, and hence its lower symmetry. In another way, structure #8 could be characterized as composed of interconnected *layered boat* structures as apparent in the view shown in Fig. 6(b). Structure #8 contains large voids in between those layers probably responsible for the less favorable enthalpy behavior at lower pressure. Structure #11 is an insulator with an indirect band gap decreasing from 2.8 eV at near zero pressure to 2.2 eV at 43 GPa. Structure #8 is also an insulator with an indirect gap at low pressures (e.g., 1.0 eV at 26 GPa) replaced by a higher energy direct gap at higher pressures (1.5 eV at 96 GPa).

In conclusion, we have described a method that systematically searches for metastable high-pressure phases of single-bonded nitrogen, by combinatorially sampling all unique distortions of a given reference structure. We demonstrate the efficiency of our method by working out in full the simplest case, the 8 atom cubic unit cell. As a result, we have found 26 new structures of single-bonded nitrogen, in addition to the previously reported single-bonded structures (CG, BP, A7, and LB). Moreover, first-principles phonon calculations show that 8 out of the 26 new structures are, in fact, metastable phases at low pressures.

The systematic search procedure presented here can be easily extended, which should lead to the discovery of even more phases. For example, the method could be extended to systematically evaluate structures of lower coordination such as that recently reported by Martin and co-workers [8], as well as structures with mixed coordination. Lower or mixed connectivity diagrams could be obtained from the original set of 36 three-coordinated diagrams by systematically breaking bonds.

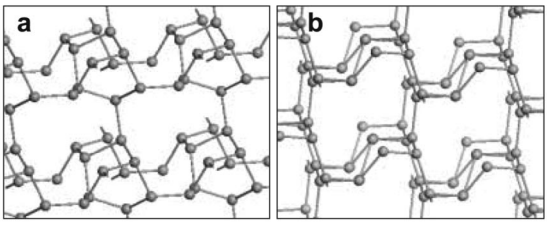

FIG. 6. Extended structures of two new low energy and metastable phases, (a) structure #11 and (b) structure #8.

The authors are grateful to Defense Research and Development Canada-Suffield and the NSERC of Canada for a financial support. Computing resources were made available by CFI, OIT, and SHARCNet of Canada.

[1] J. Uddin, V. Barone, and G. E. Scuseria, Mol. Phys. **104**, 745 (2006).
[2] C. Mailhiot, L. H. Yang, and A. K. McMahan, Phys. Rev. B **46**, 14 419 (1992).
[3] T. W. Barbee III, Phys. Rev. B **48**, 9327 (1993).
[4] M. I. Eremets, R. J. Hemley, H.-k. Mao, and E. Gregoryanz, Nature (London) **411**, 170 (2001).
[5] A. F. Goncharov, E. Gregoryanz, H.-k. Mao, Z. Liu, and R. J. Hemley, Phys. Rev. Lett. **85**, 1262 (2000).
[6] E. Gregoryanz, A. F. Goncharov, R. J. Hemley, H.-k. Mao, and M. Somayazulu, Phys. Rev. B **66**, 224108 (2002).
[7] M. I. Eremets, A. G. Gavriliuk, I. A. Trojan, D. A. Dzivenko, and R. Boehler, Nat. Mater. **3**, 558 (2004).
[8] W. D. Mattson, D. Sanchez-Portal, S. Chiesa, and R. M. Martin, Phys. Rev. Lett. **93**, 125501 (2004).
[9] M. M. G. Alemany and J. L. Martins, Phys. Rev. B **68**, 024110 (2003).
[10] F. Zahariev, A. Hu, J. Hooper, F. Zhang, and T. K. Woo, Phys. Rev. B **72**, 214108 (2005).
[11] A. F. Wells, *Three-Dimensional Nets and Polyhedra* (Wiley, New York, 1977).
[12] D. M. Adams, *Inorganic Solids* (Wiley, New York, 1974).
[13] J. K. Burdett, and T. J. McLarnan, J. Chem. Phys. **75**, 5764 (1981).
[14] J. K. Burdett, and T. J. McLarnan, J. Chem. Phys. **75**, 5774 (1981).
[15] B. Winkler, C. J. Pickard, V. Milman, and G. Thim, Chem. Phys. Lett. **337**, 36 (2001).
[16] O. D. Friedrichs, A. W. M. Dress, D. H. Huson, J. Klinowski, and A. L. Mackay, Nature (London) **400**, 644 (1999).
[17] Y. Akahama, H. Kawamura, S. Carlson, T. L. Bihan, and Hausermann, Phys. Rev. B **61**, 3139 (2000).
[18] F. Hararay, *Graph Theory* (Addison-Wesley, Reading, MA, 1994).
[19] J. P. Perdew, K. Burke, and M. Ernzerhof, Phys. Rev. Lett. **80**, 891 (1998).
[20] G. Kresse and J. Furthmuller, Phys. Rev. B **54**, 11 169 (1996).
[21] P. E. Blochl, Phys. Rev. B **50**, 17 953 (1994).
[22] See EPAPS Document No. E-PRLTAO-97-005641 for supplemental figures. For more information on EPAPS, see http://www.aip.org/pubservs/epaps.html.
[23] We have performed $3 \times 3 \times 3$ supercell phonon disperson curve calculations on BP at 38 GPa and A7 at 13 GPa and found no imaginary frequencies, although the $2 \times 2 \times 2$ supercell calculations indicate weak imaginary frequencies.